Tetrahedron: *Asymmetry* 20 (2009) 327–334

Contents lists available at ScienceDirect

Tetrahedron: *Asymmetry*

journal homepage: www.elsevier.com/locate/tetasy

Novel codeinone derivatives via Michael addition of barbituric acids

Tonko Kolev [a,*], Rumjana Bakalska [b], Rüediger W. Seidel [c], Heike Mayer-Figge [c], Iris M. Oppel [c], Michael Spiteller [a], William S. Sheldrick [c], Bojidarka B. Koleva [c]

[a] *Institut für Umweltforschung, Universität Dortmund, Otto-Hahn-Strasse 6, 44221 Dortmund, Germany*
[b] *University of Plovdiv 'P. Hilendarski', Department of Organic Chemistry, Plovdiv 4000, Bulgaria*
[c] *Lehrstuhl für Analytische Chemie, Ruhr-Universität Bochum, Universitätsstraße 150, 44780 Bochum, Germany*

ARTICLE INFO

Article history:
Received 2 December 2008
Accepted 2 February 2009
Available online 13 March 2009

ABSTRACT

Two novel adducts of codeinone with barbituric and 2-thiobarbituric acids have been synthesized via Michael addition. The compounds were spectroscopically elucidated by means of IR-LD spectroscopy of oriented samples as a suspension in nematic liquid crystals, UV spectroscopy and ^{1}H and ^{13}C NMR spectroscopy. The 2-thiobarbituric adduct was characterized by X-ray crystallography. HPLC tandem mass spectrometry (HPLC ESI MS/MS) and thermal methods were also employed. Quantum chemical calculations have been performed with a view to obtaining the electronic structure and vibrational properties of the novel compounds.

1. Introduction

The codeine derivatives are opiate agonists, exhibiting an antitussive effect, and are used to relieve mild to moderate pain.[1–3] Many of them become effective by binding to opioid receptors in the brain and spinal cord.[4] In recent years, it has been found that codeinone **1**, an oxidation product of codein, possesses antitumour potential, with high cytotoxic activity against human promyelocytic leukaemic cell lines, in addition to the reported antinociceptive activity.[5] Furthermore codeinone is an intermediary substance in the syntheses of semi-synthetic opioids such as naloxone, naltrexone, oxycodone and hydrocodone. It is known that codeinone in the living cell is produced from the reaction of codeine with nicotinamide adenine dinucleotide phosphate ($NADP^{+}$). The numerous side effects of opiate narcotics, of which physical dependence is undoubtedly the most serious, continue to stimulate the search for better analgesics.[6]

We decided to study the reactivity of the α,β-unsaturated ketone codeinone **1** towards active methylene compounds such as barbituric acid **2** and 2-thiobarbituric acid **3** via Michael addition with a view to accessing new compounds with potential biological activity (Scheme 1). The choice of the C-nucleophilic reagents was prompted by the fact that the barbiturates contain a hydrophilic functionality (2,4,6-pyrimidinetrione ring structure) and are in therapeutic use as CNS depressants (sedation, hypnotic, preanesthetic, anticonvulsant activity and headache products).[7] Such reactions have attracted interest for the preparation of compounds, which have potential utility in the field of biological chemistry. Work involving artificial, hydrogen-bonding receptors for barbiturate drugs[8] has inspired the preparation of barbiturate derivatives possessing specific host–guest recognition properties.[9] Barbiturate groups are strongly electron-withdrawing because they gain aromatic stabilization upon reduction.[10] This property has been exploited in the preparation of molecules, which possess very pronounced quadratic non-linear optical properties of interest for potential applications in opto-electronic and photonic technologies.[11,12]

A large number of reports are available on the reactions of barbituric acids with carbonyl compounds, but not so many studies on their reactions with α,β-unsaturated carbonyl systems[13,14] have appeared in the literature. Some work has been carried out on the conjugated addition reaction of C-, N-, O-, S-containing nucleophilic reagents to codeinone molecule.[15–20]

2. Results and discussion

The Michael addition of barbituric acid **2** and 2-thiobarbituric acid **3** to codeinone leads to the corresponding 8-substituted dihydrocodeinone (Scheme 1). Compounds **4a** and **5a** were identified by ^{1}H and ^{13}C NMR and mass spectrometry. The reaction gives rise to a new stereocentre at C8 with an (*S*)-configuration in addition to the stereocentres of the dihydrocodeinone moiety (5*R*,16*S*,9*R*,13*S*,14*R*). The bond distribution within the barbiturate moieties is in accordance with a formal carbanionic structure. A second new stereocentre with an (*S*)-configuration is generated at N1 of the piperidine ring of the codeine moiety due to its protonation. Thus, the compounds possess a formal zwitterionic structure. Compound **5a** was characterized by X-ray crystallography, and crystallizes in the non-centrosymmetric space group $P2_12_12_1$

* Corresponding author. Tel.: +49 0321 755 7069.
E-mail address: kolev@orgchm.bas.bg (T. Kolev).

0957-4166/$ - see front matter © 2009 Elsevier Ltd. All rights reserved.
doi:10.1016/j.tetasy.2009.02.005

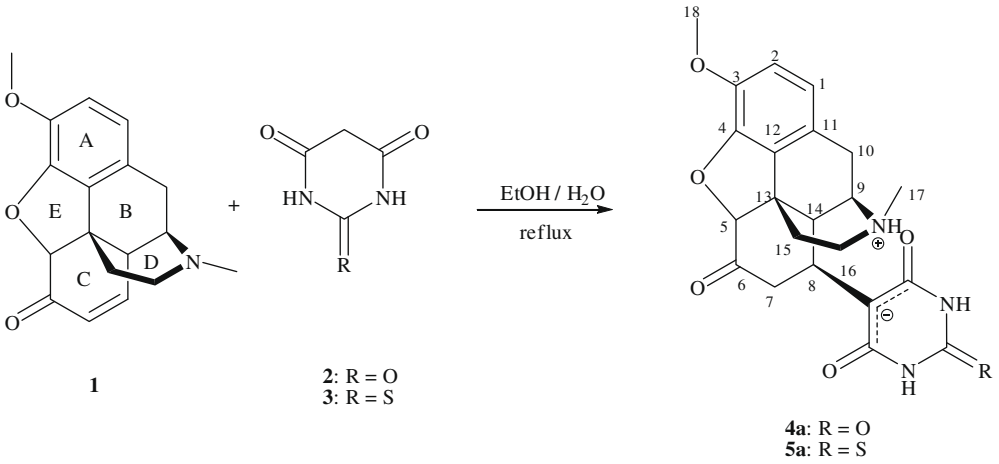

Scheme 1. Synthetic route to compounds **4a** and **5a**.

accompanied by five solvent water molecules. An ORTEP diagram is depicted in Figure 1. The dihydrocodeinone moiety exhibits the classical T-shape for opiates with a dihedral angle between the mean planes of the A/B/C and D/E rings of 81.0(4)° (Fig. 3). The rings are denoted in accordance with the commonly used nomenclature for opiates (Scheme 1). The main structural features of the molecule are very similar to those of codeine, heroin and morphine (Table 1). The ring fusion and conformations are the same as those previously reported for morphine derivatives (see Table 1). Aromatic ring A is planar, B is close to an envelope, C and D assume half-chair conformations and ring E is in a chair form. Rings A and B are effectively coplanar (Fig. 1) with a maximal deviation of only 3.1(4)° for B. Rings D and E are also mutually oriented in an approximately co-planar manner. N1 of the piperidine ring (D) forms a moderately strong N–H···O hydrogen bond to O70 of a solvent water molecule (2.745(4) Å), and O2 of the tetrahydrofuran ring (E) accepts an O–H···O hydrogen bond of a water molecule (O70) at a distance of 2.889(3) Å. The 2-thiobarbituric fragment is essentially flat with a deviation from the planarity of 0.02(1)°, and is found in the keto form as expected. The C8–C55 bond length of 1.504(3) Å is in accordance with single bond character. The C44–C55 and C55–C66 distances are 1.394(4) and 1.414(4) Å, respectively, revealing a partial double bond character. The C44–O44 and C66–O66 bond lengths of the carbonyl groups are relatively long with values of 1.267(3) and 1.254(3) Å, probably due to partial charge delocalization and hydrogen bonding. The molecules of **5a** are linked via moderately strong intermolecular hydrogen-bonding interactions between the 2-thiobarbituric acid fragments. N11 and N33 form hydrogen bonds to the carbonyl groups of an adjacent symmetry-related molecule. The N11–H11···O44 and N33–H33···O66 distances are 2.810(3) and 2.752(3) Å, respectively. O44 also accepts a hydrogen bond of length 2.766(3) Å from a water molecule (O50), and S22 accepts weak hydrogen bonds of lengths 3.225(3), 3.263(3) and 3.702(4) Å from the water molecules O50, O60 and O80, respectively. The co-crystallized solvent water molecules are all interlinked via O–H···O hydrogen bonds. The crystal structure of **4a** was also established by X-ray crystallography, and is isomorphous to that of **5a**. Although the crystals of **4a** were of poor quality, a complete structural determination (not reported) was possible (Fig. 2).

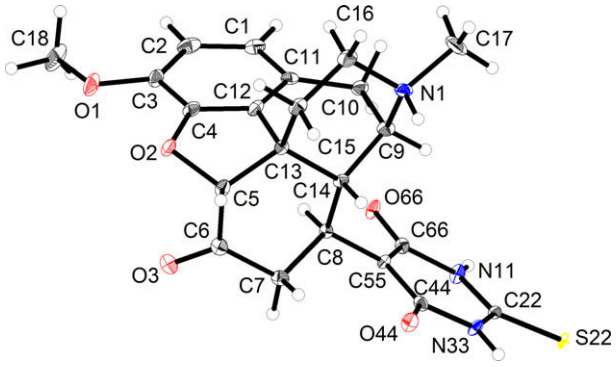

Figure 1. ORTEP diagram of **5a**. Displacement ellipsoids are drawn at the 50% probability level. Hydrogen atoms are drawn at an arbitrary size, and solvent molecules are omitted for clarity.

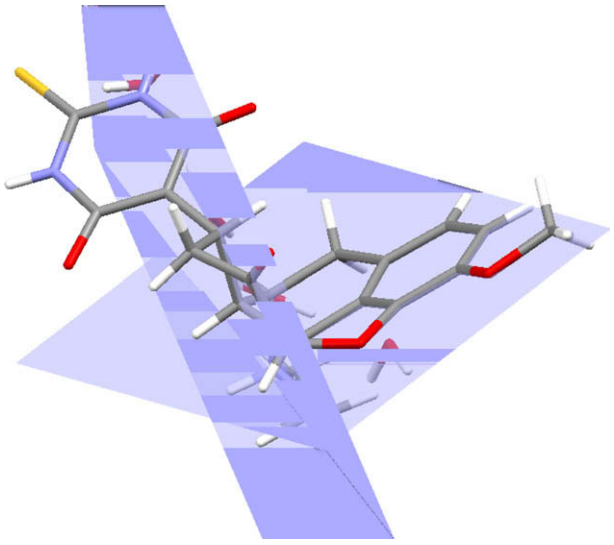

Figure 2. The dihedral angle between the mean planes of the A/B/C and D/E rings of **5a**.

On comparison of the experimental crystal structures of **5a** with those of the theoretically predicted structures (Scheme 2), a good agreement between the theoretical and experimental geometrical parameters can be established. The obtained differences of less than 0.0210 Å (**5a**) for distances as well as less than 1.7(4)° (**5a**) for bond angles indicate the suitability of the approximation and the application of the chosen theoretical approach for different codeine systems.

The absorption bands at about 260 nm (molar absorbance (ε) about 10,000 in dimension l mol^{-1} cm^{-1}) in the UV-spectra of **4a**

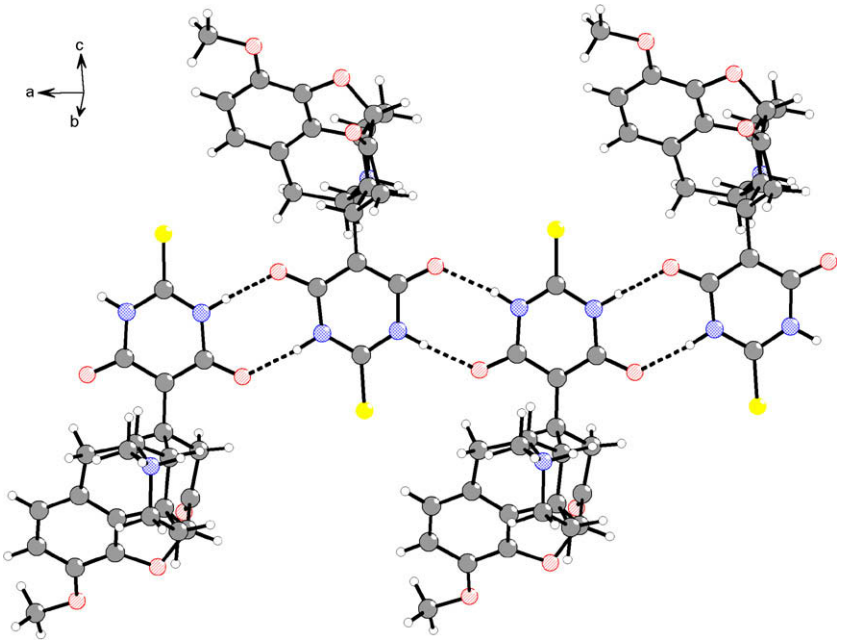

Figure 3. Intermolecular hydrogen-bonding interactions in the crystal structure of **5a**. Solvent molecules are omitted for clarity.

Table 1
Crystallographic data of the codeine and morphine derivatives, labelling using Scheme 1

R1	R2	R3	CCDC codes[a]
H	CH_3	I^-	CIMMUG[21]
	H	SO_4^-	CIMNAN[21]
		Cl^-	MORPHC[22]
		I^-	MORPHI[23]
		Br^-	ZZRHC[23]
CH_3	H	Br^-	CODHBH[24]
		Cl^-	ZZZRFQ[25]
CH_3	CH_2Cl	I^-	HAHSOY[26]
H	CH_2CHCH_2	Br^-	NALHBR[27]
		Cl^-	NALORP[28]
		I^-	FADNON[29]
β-D-Glucoron	H	—	YUJBUA[30]
CH_3	CH_3	I^-	Ref. 31

[a] CCDC—Cambridge Crystallographic Database Code, given according to the CSD version 5.29 updates (January 2008).

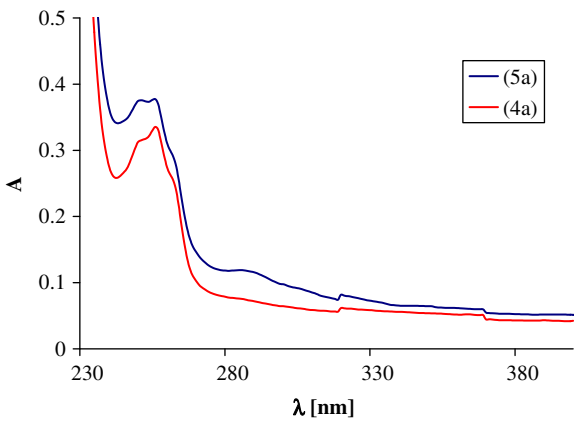

Figure 4. UV-spectra of **4a** and **5a** in acetonitrile solution.

and **5a** (Fig. 4) belong to the aromatic fragments in the molecule. An underlining bathochromic shift can be observed for **5a**, where the maximum at about 280 nm can be attributed to a CT band ($\varepsilon = 1081\ l\ mol^{-1}\ cm^{-1}$). These experimental data correlate well with our theoretical electronic spectrum, where bands at 262 nm ($f = 0.2314$) (**4a**), 260 nm ($f = 0.3332$) and 288 nm ($f = 0.072$) (**5a**) are obtained. The observed small steps in each spectrum, one at ca. 320 nm and another at ca. 370 nm, are artefacts of detector and lamp switching.

To investigate the precise geometry changes associated with the electronic excitation state, the geometries of the lowest singlet excited states of **4a** and **5a** were optimized at the CIS/6-31++G** level of theory for the comparison with the data for ground state optimized at HF/6-31++G**. The data indicate that the structural shifts are predominantly localized in the barbituric fragment in the HOMO and in the positively charged $N^+H(CH_3)$ fragment, both of which change significantly. The distributions for the HOMO and LUMO (Scheme 3) of the lowest single excited state show a strong optical emission.

Direct evidence about the stabilization of the zwitterionic structure of **4a** and **5a** in solid state can be obtained by looking at the IR-spectra of both compounds in the solid state (Fig. 5). The IR-spectroscopic region within the whole 3500–2500 cm^{-1} range is characterized by a broad strongly overlapped multicomponent band, typical for the amino acids and small peptides[32–34] and assigned to ν_{N+H} stretching vibrations. The Fermi resonance effect, observed in these discussed systems, leads to overlapping of the IR-characteristic bands within the 3050–2750 cm^{-1} region, as is typical for stretching modes of the CH_3-, CH_2- and CH-groups.[32–34] The intensive bands at about 3600 cm^{-1} and 3450 cm^{-1} belong to stretching ν_{OH} vibrations of the solvent molecules. The bands at about at 1714 cm^{-1} correspond to the stretching $\nu_{C=O}$ vibration of the codeine fragment in **4a** and **5a**, respectively. The in-plane vibrations of the aromatic fragment are observed at about 1575 cm^{-1} and 1507 cm^{-1}, and are only weakly influenced by the type of the barbituric substituent. The discussed maxima are eliminated by pairs at an equal dichroic ratio depending on their local symmetry. More significant are the differences in the IR-spectroscopic patterns of both the compounds assigned to the bending

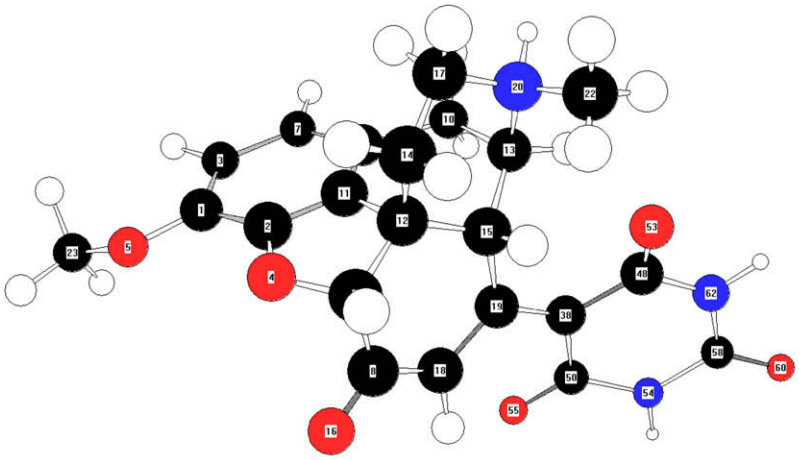

4a

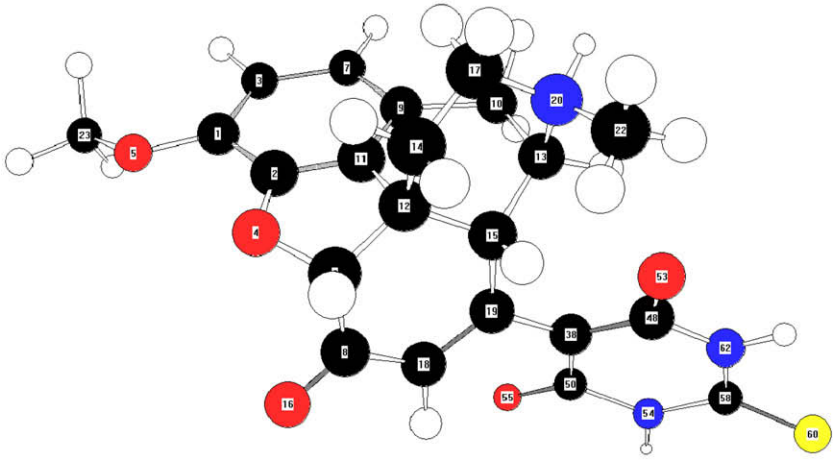

5a

Scheme 2. The theoretically most stable conformers of **4a** and **5a** and atom numbering.

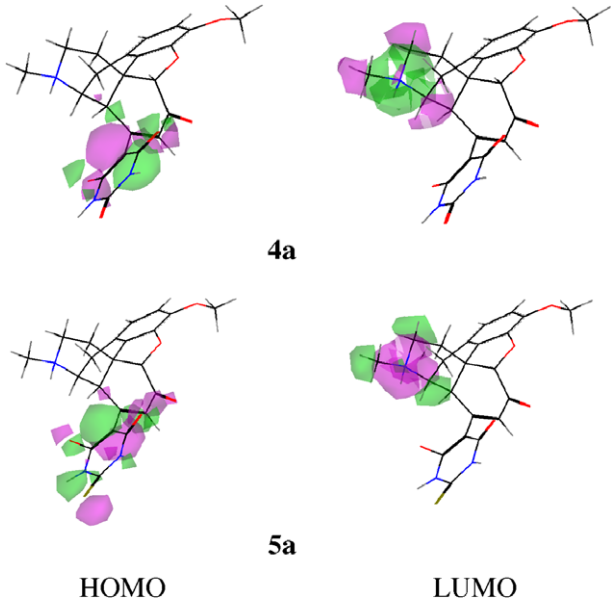

Scheme 3. Molecular orbital surface of the HOMO and LUMO for the ground state.

δ_{N+H} and δ_{NH} vibrations. According to our crystallographic data, the intermolecular interactions with participation of the discussed fragments in **4a** are stronger than those in **5a**, and for this reason,

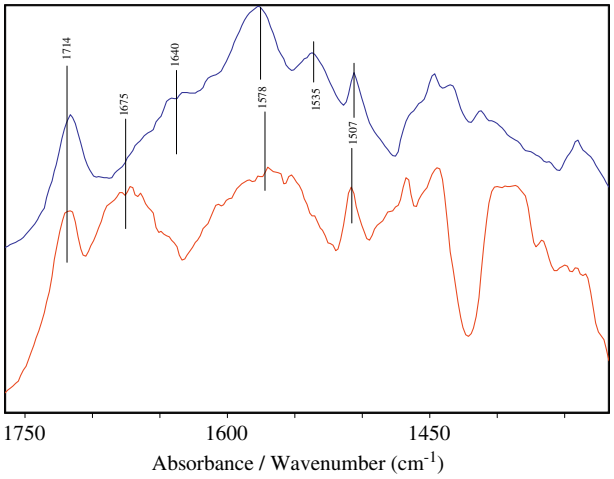

Figure 5. Solid-state IR-spectra of **4a** (1) and **5a** (2) in KBr disks.

the bending vibrations of δ_{N+H} and δ_{NH} are observed in **4a** at higher frequencies (1675 cm^{-1} and 1545 cm^{-1}) in comparison to the data of **5a** (1640 cm^{-1} and 1535 cm^{-1}).

An interesting phenomenon was observed when measuring the NMR-spectra of compounds **4a** and **5a** in DMSO-d_6 (Fig. 1).[35] Along with the signals of **4a** and **5a**, the signals of compounds **4b** and **5b** (Table 2, Scheme 4) were also discovered. This is due to the fact that adducts **4a** and **5a** in DMSO occur in two chemical structures in a hemiketal–ketoalcohol equilibrium, due to ring-chain tautomerism (Scheme 4). Structures such as **4a** and **5a**, similar to other *trans* enolizing cycloalkane-1,3-diones with four to six-membered rings, show exactly the opposite dependence on solvent polarity.[36] In these compounds, intramolecular hydrogen bonding is excluded on steric grounds, and tautomeric equilibrium seems to be controlled almost completely by the hydrogen-bond acceptor property (Lewis basicity) of the solvent. Apparently, the *trans* enolic forms are stabilized in solvent that can act as hydrogen-bond acceptor (HBA), as DMSO (Gutmann's DN = 29.8 kcal mol^{-1}, DN^N = 0.77). In the polar HBA solvent DMSO, the *trans* enolic forms are favoured.[36]

As shown in Scheme 4, the enolization of barbiturate fragments of products **4a** and **5a** in solvent with high donor properties is accompanied by conformational changes of ring C in the codeinone fragment from half-chair to boat. These conformational changes lead to spatial proximity of O4′ and C6 and favour nucleophilic addition of the alcohol function to a C-6 carbonyl group. When the hydroxyl and carbonyl groups are part of the same molecule, six-membered cyclic hemiketals **4b** and **5b** are obtained, giving rise to a new stereocentre at C*-6 with an (*S*)-configuration (Dreiding model), in addition to the previously available (5*R*, 16*S*, 9*R*, 13*S*, 14*R*) stereocentres in the codeinone fragment. The relationships of the open-chain forms to the hemiketal forms (**4a**/**4b** and **5a**/**5b**) were measured by their ^1H NMR spectra (80:20%, 4:1). For the tautomer pairs (**4a**/**4b** and **5a**/**5b**), there is a preference for the open-chain tautomers (**4a** and **5a**) over the cyclic hemiketals (**4b** and **5b**) in DMSO, such as that observed for some hydroxyketones,[37,38] but in contrast to the case of levoglucozenone.[39]

3. Conclusions

We have reported the synthesis of two novel codeinone derivatives with barbituric and thiobarbituric acids via a Michael addition. The products were characterized by NMR, UV, IR spectroscopy and mass spectrometry. Compound **5a** was also investigated by X-ray crystallography. Compound **5a** crystallizes in the non-centrosymmetric space group $P2_12_12_1$ with five co-crystallized solvent water molecules. The barbituric fragments form infinite chains by moderate strong N–H···O hydrogen-bonding interactions between the barbituric acid fragments. The molecules exhibit a T-shape with a dihedral angle between the mean planes of the A/B/C and D/E rings of 81.0(4)°. The ring fusion and conformations are the same as those previously reported for morphine derivatives. Aromatic ring A is planar, B is close to an envelope, C and D assume half-chair conformations and ring E is in a chair form. Rings A and B are effectively coplanar with a maximal deviation for B of 3.1(4)°. D and E are also mutually oriented in an approximately co-planar manner. Crystallographic and polarized IR-spectroscopic data show that the compounds are stabilized as zwitterionic structures in the solid state with deprotonated barbituric acids fragments and a protonated N^+HCH_3 function. We can also conclude that in the solid-state adducts, compounds **4a** and **5a** only occur in an open-chain form, but in DMSO solution they exist in two forms and the open-chain forms are exclusively observed. In our further investigations, we intend to study the role of solvent on the enolization, the ring-chain tautomerism and the acid–base equilibrium. On the basis of the crystal structures and their NMR (in DMSO-d_6) and IR spectra, compounds **4a** and **5a** exhibit a preference for the base form (NMe) over the conjugated base form (salt N^+HMe).

4. Experimental

4.1. Materials and synthesis

Codeine was purchased from Aldrich. Codeinone was synthesized according to the procedure described in the literature.[40]

Table 2
Some differences in the NMR spectra of the tautomer pairs **4a**/**4b** and **5a**/**5b**

Carbon/proton number	**4a** open chain	**4b** cycle	**5a** open chain	**5b** cycle
C-6	208.31	109.45	208.17	111.97
C-8	36.94	46.72	38.02	44.66
C-5′	54.86	87.26	49.05	87.04
C-4′	164.90[a] (164.66)	152.79	163.34[a] (162.84)	147.82
H-5′	3.65–3.59 m	—	3.62–3.59 m	—
OH (C-6)	—	5.69 s	—	6.00 s
H-8	1.88 dd	4.08 m	1.88 dd	3.99 m
H-5	5.10 s	5.28 m	5.10 s	5.26 m

[a] The equivalence of these carbons is caused by the close values of the two carbonyl groups at positions 2′ and 4′.

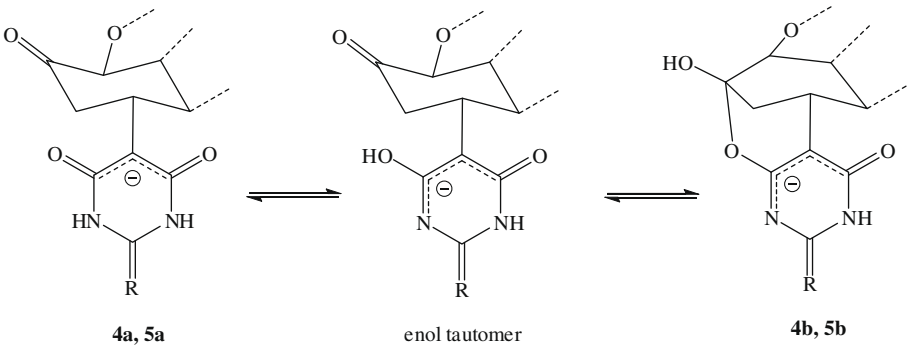

Scheme 4. Keto–enol tautomerism and intramolecular hemiketal formation of **4a** and **5a**.

The general procedures for obtaining **4a** and **5a** are as follows. *Method A:* A solution of codeinone **1** (0.093 g, 0.313 mmol) and barbituric acid **2** (0.04 g, 0.313 mmol) in abs ethanol–water (1:1, 20 ml) was heated at reflux for 5–8 h. The course of the reaction was followed by TLC. The reaction solution was allowed to cool overnight, and the crystals were separated out and dried in air. Evaporation led to the separation of more solid. Recrystallization was performed from abs ethanol–water (1:1). Yield about 90%. *Method B*:[40] Codeinone **1** (0.093 g, 0.313 mmol) was dissolved in the minimum volume of chloroform (1 ml), and was added to a solution of barbituric acid **2** (0.04 g, 0.313 mmol) in water (5 ml) at 50 °C. Crystals began to form almost immediately. The suspension was stirred at rt for 20 h, then filtered off and the white crystals were washed with water, ether and dried. Yield about 60%. Product **4a**: 5-[10-methoxy-4-methyl-14-oxo-12-oxa-4-azapentacyclo[9.6.1.0.^{1,13}0^{5,17}0^{7,18}]octadeca-7(18),8,10-trien-16-yl] hexahydro-2,4,6-pyrimidine-trione**:** $C_{22}H_{23}N_3O_6$ (M_r 425.434), mp 245.5–247 °C, $[\alpha]_D = -94.5$ (ethanol, concentration 2.5×10^{-4} mol/l and temperature 298 K) ^{1}H NMR (DMSO-d_6, 400 MHz) δ: 8.90 and 8.80 (2s, 2H, NH), 6.82 (d, 1H, J = 8.3, H-2), 6.72 (d, 1H, J = 8.3, H-1), 5.69 (s, 1H, C6–OH, cycle), 5.28 (m, 1H, H-5, cycle), 5.10 (s, 1H, H-5), 4.08 (m, 1H, H-8, cycle), 3.83 (s, 3H, CH_3O), 3.65–3.59 (m, 2H, H-9, H-5′), 3.15 (m, 1H, H-15$_{ax}$), 3.12 (dm, 1H, $J_{16eq,15ax}$ = 4.5, $J_{16eq,16ax}$ = 12.8, H-16$_{eq}$), 3.07 (dm, 1H, $J_{9,10qe}$ = 4.7, $J_{10qa,10qe}$ = 17.4, H-10$_{qe}$), 3.02 (m, 1H, H-10$_{qa}$), 2.83 (s, 3H, NCH_3), 2.63 (t, 1H, $J_{8ax,14}$ = 11.2, $J_{9,14}$ = 2.3, H-14), 2.20 (m, 1H, H-7$_{ax}$), 1.88–1.85 (dd, 1H, $J_{8ax,7ax}$ = 15.8, $J_{8ax,14}$ = 11.2, $J_{8ax,7eq}$ = 2.4, $J_{8ax,5'}$ = 13.7, H-8$_{ax}$), 1.74 (dm, 1H, $J_{7ax,7eq}$ = 12.1, H-7$_{eq}$), 1.23 (s, 1H, H-15$_{eq}$). The signal of proton H-16$_{ax}$ (2.49) overlaps with the DMSO signal. ^{13}C NMR (DMSO-d_6, 101 MHz): 208.31 (C-6), 164.90, 164.66 (C-4′, C-6′), 152.79 (C-4′, cycle), 152.45 (C-2′), 145.44 (C-4), 142.91 (C-3), 135.19 (C-12), 126.95 (C-11), 120.47 (C-1), 115.62 (C-2), 109.45 (C-6 cycle) 90.88 (C-5), 87.26 (C-5′ cycle), 79.34 (C-9), 79.01 (C-14), 56.91 (CH_3O), 55.13 (NCH_3), 54.86 (C-5′), (C-16), 54.58 (C-16), 46.72 (C-8, cycle), 45.82 (C-13), 33.29 (C-7), 32.53 (C-15), 27.94 (C-8), 26.16 (C-10); UV [EtOH–H_2O, 1:1] λ_{max}, nm: 260.8 (1.903 Å), 226.4 (1.342 Å), 206.0 (2.123 Å). Product **5a**: $C_{22}H_{23}N_3O_5S$ (M_r 441.500), yield 0.104 g (76%), mp >330 °C, $[\alpha]_D = -92.3$ (ethanol, concentration 2.5×10^{-4} mol/l and temperature 298 K); ^{1}H NMR (DMSO-d_6, 400 MHz) δ: 10.40 (d, 1H, J = 15.4, NH), 8.40 (m, 1H, NH), 6.83 (d, 1H, J = 8.3, H-2), 6.74 (d, 1H, J = 8.3, H-1), 6.00 (s, 1H, C6–OH, cycle), 5.26 (m, 1H, H-5, cycle), 5.10 (s, 1H, H-5), 3.99 (m, 1H, H-8 cycle), 3.83 (s, 3H, CH_3O), 3.62–3.59 (m, 2H, H-9, H-5′), 3.14 (dm, 2H, $J_{8ax,14}$ = 11.3, H-14, H-16$_{eq}$), 3.06–2.98 (br s, 2H, H-10$_{qe}$, H-16$_{ax}$), 2.82 (s, 3H, NCH_3), 2.63 (t, 2H, $J_{10qa,10qe}$ = 18.4, $J_{15ax,16ax}$ = 12.0, $J_{15ax,16ax}$ = 11.3, H-10$_{qa}$, H-15$_{ax}$), 2.20 (m, 1H, H-7$_{ax}$), 1.88–1.86 (dd, 2H, $J_{8ax,7ax}$ = 15.8, $J_{8ax,7eq}$ = 2.3, $J_{15eq,15ax}$ = 13.5, $J_{15eq,16eq}$ = 1.1, H-8$_{ax}$, H-15$_{eq}$), 1.74 (dm, 1H, $J_{7ax,7eq}$ = 12.3, H-7$_{eq}$); ^{13}C NMR (DMSO-d_6, 101 MHz): ^{13}C NMR (DMSO-d_6, 101 MHz): 208.17 (C-6), 163.34, 162.84 (C-4', C-6′), 173.42 (C-2′), 147.82 (C-4′, cycle), 145.35 (C-4), 142.94 (C-3), 126.64 (C-12), 124.59 (C-11), 120.63 (C-1), 115.61 (C-2), 111.97 (C-6 cycle) 90.77 (C-5), 87.04 (C-5′ cycle), 60.40 (C-9), 56.84 (CH_3O) 49.05 (C-5'), 47.30 (NCH_3), 44.85 (C-16), 44.69 (C-14), 44.66 (C-8, cycle), 44.35 (C-13), 40.33 (C-7), 38.02 (C-8), 32.18 (C-15), 21.22 (C-10); UV [EtOH–H_2O, 1:1] λ_{max}, nm: 284.8 (1.071 Å), 268.0 (0.998 Å), 232.8 (0.779 Å), 206.4 (2.033 Å).

Adducts of codeinone **1** and barbituric acid **2** or 2-thiobarbituric acid **3** (Scheme 1) were prepared using a simple one-pot procedure. Equimolar amounts of ketone **1** and the appropriate barbituric acid were heated at reflux in abs ethanol–water (1:1) (method A) for 5–8 h. The corresponding products, compounds **4a** and **5a,** exhibit low solubility and precipitate in good yields as colourless crystal upon cooling of the reaction mixture. Various solvents such as acetonitrile and the two-phase systems chloroform–water and 1,4-dioxane–water were also screened for this reaction. However, the best results and single crystals appropriate for X-ray analysis were observed using the solvent mixtures abs ethanol–water (1:1). When the same reactions were carried out in the two-phase system chloroform–water (method B),[21] a suspension of codeinone barbiturate salts appeared immediately. It was necessary to carry out the reaction for 20 h with more intensive stirring of the reaction mixture at room temperature to obtain the products **4a** and **5a** in yields of about 60%, and in this manner they were obtained as fine powders.

4.2. Materials and methods

The X-ray diffraction intensities were recorded on an Oxford Diffraction Xcalibur2 diffractometer equipped with a Sapphire2 CCD detector and graphite-monochromatized Cu Kα radiation. The data were corrected for Lorentz and polarization effects. A semi-empirical absorption correction based on multiple scanned reflections was performed with ABSPACK implemented in CRYSALIS RED.[41] The crystal structure was solved by direct methods using SHELXS-97 and refined by full-matrix least-squares refinement on F^2 using SHELXL-97.[42] Anisotropic displacement parameters were introduced for all non-hydrogen atoms. The oxygen atoms of the solvent water exhibited high thermal parameters. Hydrogen atoms bonded to carbon and nitrogen were placed at geometrically calculated positions and refined with the appropriate riding model. The positions of the hydrogen atoms attached to nitrogen were confirmed from the difference map. The water hydrogen atoms were located in a difference Fourier synthesis and refined with restrained O–H distance (0.84(2) Å) and isotropic temperature factors of 1.2 times of the parent oxygen atom. The 1,3-H–H distance of H80A and H80B was restrained to 1.42(2) Å. The absolute configuration of the molecule was confirmed by the Flack parameter (−0.02(2)).[43] Relevant crystallographic data and refinement details are given in Table 3, and selected bond length and angles in Table 4.

Conventional and polarized IR-spectra were measured on a Thermo Nicolet 6700 FTIR-spectrometer (4000–400 cm^{-1}, 2 cm^{-1} resolution, 200 scans) equipped with a Specac wire-grid polarizer. Non-polarized solid-state IR spectra were recorded using the KBr disk technique. The oriented samples were obtained as a colloid suspension in a nematic liquid crystal ZLI 1695. The theoretical ap-

Table 3
Crystal and refinement data for **5a**

Empirical formula	$C_{22}H_{23}N_3O_5S{\cdot}5H_2O$
M_r	531.57
T (K)	108(2)
λ (Å)	1.54184
Crystal system, space group	Orthorhombic, $P2_12_12_1$
a (Å)	11.8563(2)
b (Å)	12.9471(2)
c (Å)	15.9563(2)
V (Å^3)	2449.37(6)
Z	4
ρ (mg m^{-3})	1.442
μ (mm^{-1})	1.719
F(000)	1128
Crystal size (mm)	0.13 × 0.11 × 0.10
θ Range for data collection (°)	4.4 ⩽ θ ⩽ 65.64
Limiting indices	−13 ⩽ h ⩽ 12, −15 ⩽ k ⩽ 12, −17 ⩽ l ⩽ 18
Reflections collected/unique	12,586/3992
R_{int}	0.0414
Refined parameters/restraints	357/11
Goodness-of-fit on F^2	0.843
R_1 ($I > 2\sigma(I)$)	0.0340
wR_2 (all data)	0.0665
Residuals (e Å^{-3})	0.238/−0.323

Table 4
Selected bond lengths (Å) and angles (°) of **5a**

S1 C20 1.704(3)	C16 C6 1.545(4)	C15 N1 C6 112.4(2)	C22 C10 C3 113.3(3)
O5 C21 1.271(4)	C15 C5 1.517(5)	N31 C20 N2 116.7(3)	C22 C10 C8 113.6(3)
N31 C20 1.335(4)	C14 C8 1.492(5)	N31 C20 S1 120.6(3)	C3 C10 C8 106.9(3)
N31 C21 1.410(4)	C14 C9 1.526(5)	N2 C20 S1 122.7(3)	O2 C9 C14 107.5(3)
O4 C19 1.374(4)	C13 C11 1.394(5)	O4 C19 C18 117.5(3)	O2 C9 C4 105.0(2)
O4 C1 1.474(3)	C10 C3 1.535(4)	O4 C19 C11 126.0(3)	C14 C9 C4 113.1(3)
C22 C21 1.388(5)	C10 C8 1.547(4)	C18 C19 C11 116.5(3)	C14 C8 C10 110.4(3)
C22 C12 1.413(5)	C9 C4 1.547(4)	C7 C18 C19 121.3(3)	C18 C7 C17 123.5(3)
C22 C10 1.507(4)	C7 C4 1.508(5)	C7 C18 O2 111.9(3)	C18 C7 C4 109.7(3)
O3 C12 1.255(4)	C6 C3 1.545(4)	C19 C18 O2 126.7(3)	C17 C7 C4 126.7(3)
N2 C20 1.335(4)	C5 C4 1.533(4)	C7 C17 C13 115.8(3)	N1 C6 C3 106.2(3)
N2 C12 1.406(4)	C4 C3 1.543(4)	C7 C17 C16 118.1(3)	N1 C6 C16 113.2(3)
O2 C18 1.396(4)	C20 N31 C21 124.2(3)	C13 C17 C16 125.7(3)	C3 C6 C16 114.9(3)
O2 C9 1.478(4)	C19 O4 C1 116.4(2)	C17 C16 C6 114.6(3)	C15 C5 C4 111.2(3)
O1 C14 1.216(4)	C21 C22 C12 119.3(3)	N1 C15 C5 109.9(3)	C7 C4 C5 111.2(3)
N1 C2 1.485(4)	C21 C22 C10 122.3(3)	O1 C14 C8 123.4(3)	C7 C4 C3 108.5(3)
N1 C15 1.514(4)	C12 C22 C10 118.4(3)	O1 C14 C9 120.6(3)	C5 C4 C3 109.4(3)
N1 C6 1.529(4)	C20 N2 C12 124.8(3)	C8 C14 C9 116.0(3)	C7 C4 C9 98.5(3)
C19 C18 1.382(5)	C18 O2 C9 104.2(2)	C17 C13 C11 121.5(3)	C5 C4 C9 111.0(3)
C19 C11 1.400(5)	O5 C21 C22 126.0(3)	O3 C12 N2 117.6(3)	C3 C4 C9 117.7(3)
C18 C7 1.369(5)	O5 C21 N31 116.0(3)	O3 C12 C22 125.5(3)	C10 C3 C4 111.9(3)
C17 C7 1.380(5)	C22 C21 N31 117.9(3)	N2 C12 C22 116.9(3)	C10 C3 C6 113.9(3)
C17 C13 1.389(5)	C2 N1 C15 111.6(3)	C13 C11 C19 121.4(3)	C4 C3 C6 106.1(3)
C17 C16 1.512(4)	C2 N1 C6 114.3(3)		

proach, as well as the experimental technique for preparing the samples and procedures for polarized IR-spectra interpretation and the validation of this new linear-dichroic infrared (IR-LD) orientation solid-state method for accuracy and precision have been presented previously. The influence of the liquid crystal medium on the peak positions and integral absorbances of the guest molecule bands, the reological model, the nature and balance of the forces in the nematic liquid crystal suspension system and the morphology of the suspended particles have also been discussed.[44–47]

The positive and negative FAB mass spectra were recorded on a Fisons VG Autospec instrument employing 3-nitrobenzylalcohol (Sigma–Aldrich) as the matrix.

Ultraviolet (UV-) spectra were recorded on Tecan Safire Absorbance/Fluorescence XFluor 4 V 4.40 spectrophotometer operating between 190 and 900 nm, using solvent acetonitrile (Uvasol, Merck product) at a concentration of 2.5×10^{-5} M in 0.921 cm quartz cells.

Quantum chemical calculations were performed with the GAUSSIAN 98 and DALTON 2.0 program packages,[48,49] and the output files were visualized by means of the CHEMCRAFT program.[50] The geometries of the compounds **4a** and **5a** were optimized at two levels of theory: second-order Moller–Pleset perturbation theory (MP2) and density functional theory (DFT) using the 6-31+G** basis set. The DFT method employed is B3LYP, which combines Backe's three-parameter non-local exchange function with the correlation function of Lee, Yang and Parr. Molecular geometries of the studied species were fully optimized by the force gradient method using Bernys' algorithm. For every structure, the stationary points found on the molecule potential energy hypersurfaces were characterized using standard analytical harmonic vibrational analysis. The absence of the imaginary frequencies, as well as of negative eigenvalues of the second-derivative matrix, confirmed that the stationary points correspond to minima of the potential energy hypersurfaces. The calculation of vibrational frequencies and infrared intensities was checked to establish which kind of performed calculations agreed best with the experimental data. As a result, the B3LYP/6-31++G** and MP2/6-31++G** data are presented for the above-discussed modes, where a modification of the results using the empirical scaling factors 0.9614 and 0.8929 is made to achieve better correspondence between the experimental and theoretical values. The UV spectra in the gas phase and in acetonitrile solution were obtained by CIS/6-31++G** and TDDFT calculations.

The thermal analyses were performed in the 300–500 K range on a Differential Scanning Calorimeter Perkin–Elmer DSC-7 and a Differential Thermal Analyzer DTA/TG (Seiko Instrument, model TG/DTA 300). The experiments were carried out with a scanning rate of 10 K min^{-1} under an argon atmosphere.

The *elemental analysis* was carried out according to the standard procedures for C and H (as CO_2, and H_2O) and N (by the Dumas method).

The *melting points* were measured on Kofler apparatus and were uncorrected. The TLC was performed on plates of Silica Gel 60 (Merck) with EtOH–H_2O–concd NH_4OH (100:6:4) as the mobile phase.

5. Crystallographic data

Crystallographic data for the structural analysis have been deposited with the Cambridge Crystallographic Data Centre, CCDC 711681. Copies of this information may be obtained from the Director, CCDC, 12 Union Road, Cambridge, CB2 1EZ, UK (Fax: +44 1223 336 033; e-mail: deposit@ccdc.cam.ac.uk or http://www.ccdc.cam.ac.uk).

Acknowledgements

B.K. wishes to thank the Alexander von Humboldt Foundation for a Fellowship, T.K. and M.S. the DAAD for a grant within the priority program 'Stability Pact South-Eastern Europe' and the Alexander von Humboldt Foundation.

References

1. Erichsen, H. K.; Hao, J. X.; Xu, X. J. *Pain* **2005**, *116*, 347.
2. Gonenne, J.; Ferber, I.; Burton, D. *Gastroenterology* **2005**, *28*, A94.
3. Gruss, H. J.; Sutton, A.; Horton, P. *Gastroenterology* **2005**, *128*, A465.
4. Neri, C.; Guarna, M.; Blanchi, E. *Med. Sci. Monitor* **2004**, *10*, MS1.
5. Hitosugi, N.; Hatsukari, I.; Ohno, R.; Hashimoto, K.; Mihara, S.; Mizukami, S.; Nakamura, S.; Sakagami, H.; Nagasaka, H.; Matsumoto, I.; Kawase, M. *Anesthesiology* **2003**, *98*, 643.
6. Anathan, S.; Khare, N. K.; Saini, S. K.; Seitz, L. E.; Barlett, J. L.; Davis, P.; Dersch, C. M.; Porreca, F.; Rothman, R. B.; Bilsky, E. J. *J. Med. Chem.* **2004**, *47*, 1400.
7. Gringauz, A. *Introduction to Medicinal Chemistry—How Drugs Act and Why*; Wiley-VCH: New York, 1997.

8. Koike, T.; Takashige, M.; Kimura, E.; Fujioka, H.; Shiro, M. *Chem. Eur. J.* **1996**, *2*, 617.
9. Chin, T.; Gao, Z.; Lelouche, I.; Shin, K.; Purandare, A.; Knapp, S.; Isied, S. *J. Am. Chem. Soc.* **1997**, *119*, 12849.
10. Marder, S. R.; Beratan, D. N.; Cheng, L.-T. *Science* **1991**, 252.
11. Marder, S. R.; Cheng, L.-T.; Tiemann, B. G.; Friedli, A. C.; Blanchard-Desce, M.; Perry, J. W.; Skindhøj, J. *Science* **1994**, *263*, 511.
12. Adamson, J.; Coe, B. J.; Grassam, H. L.; Jeffery, J. C.; Coles, S. J.; Hursthouse, M. B. *J. Chem. Soc., Perkin Trans. 1* **1999**, 2483.
13. Mskwin, A. B.; Reznikova, H. P. *J. Org. Chem.* **2002**, *38*, 487.
14. Ahmed, M. G.; Romman, U. K. R.; Ahmed, S. M.; Akhter, K.; Halim, M.; Salauddin, M. *Bang. J. Sci. Ind. Res.* **2006**, *41*, 119.
15. King, W.; Penprase, W. G.; Kloetzel, M. C. *J. Org. Chem.* **1961**, *26*, 3558.
16. Seki, I. *Chem. Pharm. Bull.* **1970**, *18*, 671.
17. Kotick, M. P.; Leland, D. L.; Polazzi, J. O.; Schut, R. N. *J. Med. Chem.* **1980**, *23*, 166.
18. Kotick, M. P.; Polazzi, J. O. *J. Heterocycl. Chem.* **1981**, *18*, 1029.
19. Kotick, M. P. *J. Med. Chem.* **1981**, *24*, 722.
20. Chozland, F.; Maroni, P.; Viloria, I.; Cros, I. *Eur. J. Med. Chem.—Chim. Ther.* **1983**, 18.
21. Wongweichintana, C.; Holt, E. M.; Purdie, N. *Acta Crystallogr., Sect. C* **1984**, *40*, 1486.
22. Gylbert, L. *Acta Crystallogr., Sect. B* **1973**, *29*, 1630.
23. Mackay, M.; Hodgkin, D. C. *J. Chem. Soc.* **1955**, 3261.
24. Kartha, G.; Ahmed, F. R.; Barnes, W. H. *Acta Crystallogr.* **1962**, *15*, 326.
25. Barnes, L. *Can. J. Chem.* **1955**, *33*, 565.
26. Grant, A.; Zacharias, D.; Mascavage, L.; Kemmerer, G.; Dalton, D. *J. Heterocycl. Chem.* **1993**, *30*, 553.
27. Gelders, Y. G.; De Ranter, C. J.; van Rooijen-Reiss, C. *Cryst. Struct. Commun.* **1979**, *8*, 995.
28. Duchamp, D. J.; Olson, E. C.; Chidester, C. G. *ACA, Ser. 2* **1977**, *5*, 83.
29. Kobylecki, R. J.; Lane, A. C.; Smith, C. F. C.; Wakelin, L. P. G.; Cruse, W. B. T.; Egert, E.; Kennard, O. *J. Med. Chem.* **1986**, *29*, 1278.
30. Urbanczyk-Lipkowska, Z. *Acta Crystallogr., Sect. C* **1995**, *51*, 1184.
31. Seidel, R. W.; Bakalska, B.R.; Kolev, T.; Vassilev, D.; Mayer-Figge, H.; Spiteller, M.; Sheldrick, W.S.; Koleva, B.B. *Spectrochim. Acta, Part A*, submitted for publication.
32. Ivanova, B. B.; Kolev, T.; Zareva, S. Y. *Biopolymers* **2006**, *82*, 587.
33. Koleva, B. B.; Kolev, T. M.; Spiteller, M. *Biopolymers* **2006**, *83*, 498.
34. Koleva, B. B.; Kolev, Ts.; Spiteller, M. *Inorg. Chim. Acta* **2007**, *360*, 2224.
35. Bakalska, R. I.; Chervenkova, V. B.; Venkov, A. *Scientific Works—Chem.* **2000**, *29*, 67.
36. Reichardt, C. *Solvents and Solvent Effects in Organic Chemistry*, 3rd ed.; Wiley-VCH Verlag GmbH, 2003.
37. Whiting, J. E.; Edward, J. T. *Can. J. Chem.* **1971**, *49*, 3799.
38. Langhals, H. *Angew. Chem.* **1982**, *94*, 739.
39. Samet, A. V.; Yamskov, A. N.; Ugrak, B. I.; Semenov, V. V. *Russ. Chem. Bull.* **1997**, *46*, 532.
40. Bakalska, R. I.; Chervenkova, V. B. *Bulg. Chem. Ind.* **2002**, *73*, 108.
41. CRYSALIS RED, Version 1.171.32.11, Oxford Diffraction Ltd.
42. Sheldrick, G. M.; *Acta Crystallogr., Sect. A.* **2008**, *64*, 112.
43. Flack, H. D. *Acta Crystallogr., Sect. A* **1983**, *39*, 876.
44. Ivanova, B. B.; Arnaudov, M. G.; Bontchev, P. R. *Spectrochim. Acta, Part A* **2004**, *60*, 855.
45. Ivanova, B. B.; Tsalev, D. L.; Arnaudov, M. G. *Talanta* **2006**, *69*, 822.
46. Ivanova, B.; Simeonov, V.; Arnaudov, M.; Tsalev, D. *Spectrochim. Acta, Part A* **2007**, *67*, 66.
47. Koleva, B. B.; Kolev, T. M.; Simeonov, V.; Spassov, T.; Spiteller, M. *J. Inclus. Prenome*. **2008**. doi:10.1007/s10847-008-9425-5.
48. Frisch, M. J.; Trucks, G. W.; Schlegel, H. B.; Scuseria, G. E.; Robb, M. A.; Cheeseman, J. R.; Zakrzewski, V. G.; Montgomery, J. A., Jr.; Stratmann, R. E.; Burant, J. C.; Dapprich, S.; Millam, J. M.; Daniels, A. D.; Kudin, K. N.; Strain, M. C.; Farkas, Ö.; Tomasi, J.; Barone, V.; Cossi, M.; Cammi, R.; Mennucci, B.; Pomelli, C.; Adamo, C.; Clifford, S.; Ochterski, J.; Petersson, G. A.; Ayala, P. Y.; Cui, Q.; Morokuma, K.; Salvador, P.; Dannenberg, J. J.; Malick, D. K.; Rabuck, A. D.; Raghavachari, K.; Foresman, J. B.; Cioslowski, J.; Ortiz, J. V.; Baboul, A. G.; Stefanov, B. B.; Liu, G.; Liashenko, A.; Piskorz, P.; Komáromi, I.; Gomperts, R.; Martin, R. L.; Fox, D. J.; Keith, T.; Al-Laham, M. A.; Peng, C. Y.; Nanayakkara, A.; Challacombe, M.; Gill, P. M. W.; Johnson, B.; Chen, W.; Wong, M. W.; Andres, J. L.; Gonzalez, C.; Head-Gordon, M.; Replogle, E. S.; Pople, J. A. GAUSSIAN 98, Gaussian: Pittsburgh, PA, 1998.
49. 'DALTON', a molecular electronic structure program, Release 2.0, 2005, http://www.kjemi.uio.no/software/dalton/dalton.html.
50. Zhurko, G. A.; Zhurko, D. A. ChemCraft: Tool for treatment of chemical data, Lite version build 08, 2005.